Article:

Dong, Y.-Y., Dong, C.-X., Liu, W. orcid.org/0000-0003-2968-2888 et al. (1 more author) (2020) DOA estimation with known waveforms in the presence of unknown time delays and Doppler shifts. Signal Processing, 166. 107232. ISSN 0165-1684

https://doi.org/10.1016/j.sigpro.2019.07.025

DOA Estimation with Known Waveforms in the Presence of Unknown Time Delays and Doppler Shifts

Yang-Yang Dong[a,*], Chun-Xi Dong[a], Wei Liu[b], Ming-Ming Liu[a]

[a] *School of Electronic Engineering, Xidian University, Xi'an 710071, China*
[b] *Department of Electronic and Electrical Engineering, University of Sheffield, S1 4ET, U.K.*

Abstract

A novel DOA estimation method for known waveform sources with different unknown time delays and Doppler shifts is proposed. Based on the idea of maximum likelihood and the matrix projection theory, a decoupled cost function is first constructed and then the problem of estimating time delay and Doppler shift is transformed into a nonlinear least squares (NLS) problem. To solve the NLS problem efficiently without multidimensional search, a Toeplitz dominant rule is established to perform initial estimates with a reduced dimension. Finally, with the aid of time delay and Doppler shift estimates, DOAs and complex amplitudes of the incoming signals are obtained. Simulation results show that the proposed method can achieve a performance close to CRB at high SNR and with a large number of snapshots.

Keywords: Direction of arrival estimation, known waveform, time delay, Doppler shift.

*Corresponding author
Email address: `dongyangyang2104@126.com` (Yang-Yang Dong)

1. Introduction

Direction of arrival (DOA) estimation is a widely studied problem in wireless communications, radar, and sonar, etc [1]. Various DOA estimation methods, such as subspace-based methods [2–5], and sparsity-inducing methods [6–8], have been developed. These methods are mainly realized on the assumption that the received signals are either unknown deterministic or random. However, for many real applications, such as communications [9] and radar [10], prior information of the signal waveform can be acquired. With the aid of waveform information, a better angle estimation performance can be achieved [11]. Hence, many methods have been developed to deal with DOA estimation for known waveform sources [11–24]. Most existing methods, such as DEML [12], SB [14], LR [17], CDEML [19], and LP [22], assume that the known waveforms arrive at the same time. However, in practice, they may arrive with different unknown time delays and Doppler shifts. A couple of methods [13, 24] have been proposed to deal with either of the two aforementioned problems, i.e., either with unknown time delays [13] or with unknown Doppler shifts [24]. Apart from the work in [10], which deals with a single known waveform with multiple multipath signals in the presence of unknown time delays and Doppler shifts, to our best knowledge, there has not been any work for DOA estimation for multiple known waveform sources in the presence of unknown time delays and Doppler shifts.

In this work, the DOA estimation problem for multiple known waveform sources in the presence of unknown time delays and Doppler shifts is investigated for the first time, and a new DOA estimation model incorporating the time delay and Doppler effect is established first. Then, based on the idea of maximum likelihood and the matrix projection theory, a decoupled cost function is constructed, where estimation of the time delay and Doppler shift is transformed into a nonlinear least squares (NLS) problem. To solve the NLS problem efficiently, a Toeplitz dominant rule is employed to provide initial estimates with a reduced dimension. Finally, with the estimated time delay and Doppler shift, the DOA and complex amplitude information is obtained based on the data structure. Simulation results show that the estimation performance of the proposed method can achieve the Cramer-Rao Bound (CRB) at high SNR and with a large number of snapshots in the presence of unknown time delays and Doppler shifts.

The rest of the paper is organised as follows. In Section 2, the studied signal model along with some necessary assumptions is introduced. The proposed method is derived in Section 3. Simulation results are provided in Section 4 and conclusions are drawn in Section 5.

Notations: matrices and vectors are denoted by bold upper-case and lower-case letters, respectively. $(\cdot)^*$, $(\cdot)^T$ $(\cdot)^H$, $(\cdot)^{-1}$, and $(\cdot)^\dagger$ stand for conjugate, transpose, conjugate transpose, inverse, and Moore-Penrose inverse, respectively. $\circ$, $\otimes$, diag$\{\cdot\}$, vec$\{\cdot\}$, tr$\{\cdot\}$, $\|\cdot\|_F$, $\|\cdot\|_2$, and angle$\{\cdot\}$ denote the Hadamard product, Kronecker product, diagonalization, vectorization, trace, Frobenius norm, ℓ_2 norm, and phase of a complex number, respectively. $\mathbf{I}_N$ is the identity matrix of size N.

2. Signal Model

Consider an M-element uniform linear array (ULA) with inter-sensor spacing d. Q narrowband far-field uncorrelated sources with known waveforms $\{s_q(n)\}_{q=1}^{Q}$ ($n = 0, \cdots, N-1$ with N being the number of snapshots) of wavelength λ from distinct directions $\{\theta_q\}_{q=1}^{Q}$ (unknown) impinge on the array. Due to the asynchronous effect and relative movement, the signal received by the mth element ($m = 1, \cdots, M$) can be expressed as

$$x_m(n) = \sum\nolimits_{q=1}^{Q} a_m(\theta_q)\gamma_q e^{j2\pi f_{Dq}n} s_q(n-\tau_q) + w_m(n) \tag{1}$$

where $a_m(\theta_q) = \exp[-j2\pi(m-1)d\sin\theta_q/\lambda]$, γ_q denotes the complex amplitude of the received qth known waveform signal, f_{Dq} denotes the Doppler shift of the qth signal resulting from the relative movement of the source to the ULA, τ_q denotes the time delay of the qth signal resulting from asynchronous receiving, and $w_m(n)$ is the noise.

The received signal vector at the nth snapshot can be represented by

$$\mathbf{x}(n) = \mathbf{A}(\theta)\boldsymbol{\Gamma}(\boldsymbol{\gamma})(\mathbf{s}_D(\mathbf{f}_D, n) \circ \mathbf{s}_\tau(n)) + \mathbf{w}(n) \tag{2}$$

$$= \mathbf{B}(\boldsymbol{\theta}, \boldsymbol{\gamma})(\mathbf{s}_D(\mathbf{f}_D, n) \circ \mathbf{s}_\tau(n)) + \mathbf{w}(n) \tag{3}$$

where

$$\begin{aligned}
\mathbf{x}(n) &= [x_1(n), x_2(n), \cdots, x_M(n)]^T, \\
\mathbf{B}(\boldsymbol{\theta}, \boldsymbol{\gamma}) &= \mathbf{A}(\boldsymbol{\theta})\boldsymbol{\Gamma}(\boldsymbol{\gamma}), \\
\mathbf{A}(\boldsymbol{\theta}) &= [\mathbf{a}(\theta_1), \mathbf{a}(\theta_2), \cdots, \mathbf{a}(\theta_Q)], \\
\mathbf{a}(\theta_q) &= [a_1(\theta_q), a_2(\theta_q), \cdots, a_M(\theta_q)], \\
\boldsymbol{\Gamma}(\boldsymbol{\gamma}) &= \mathrm{diag}\{\gamma_1, \gamma_2, \cdots, \gamma_Q\}, \\
\mathbf{s}_D(\mathbf{f}_D, n) &= [e^{j2\pi f_{D1} n}, e^{j2\pi f_{D2} n}, \cdots, e^{j2\pi f_{DQ} n}]^T, \\
\mathbf{s}_{\boldsymbol{\tau}}(n) &= [s_1(n-\tau_1), s_2(n-\tau_2), \cdots, s_Q(n-\tau_Q)]^T, \\
\mathbf{w}(n) &= [w_1(n), w_2(n), \cdots, w_M(n)]^T, \\
\boldsymbol{\theta} &= [\theta_1, \theta_2, \cdots, \theta_Q]^T, \\
\boldsymbol{\gamma} &= [\gamma_1, \gamma_2, \cdots, \gamma_Q]^T,
\end{aligned}$$

$$\begin{aligned}
\mathbf{f}_D &= [f_{D1}, f_{D2}, \cdots, f_{DQ}]^T, \\
\boldsymbol{\tau} &= [\tau_1, \tau_2, \cdots, \tau_Q]^T.
\end{aligned}$$

With a total number of N snapshots, in matrix form, we have

$$\mathbf{X} = \mathbf{B}(\boldsymbol{\theta}, \boldsymbol{\gamma})(\mathbf{S}_D(\mathbf{f}_D) \circ \mathbf{S}(\boldsymbol{\tau})) + \mathbf{W} \tag{4}$$

where

$$\begin{aligned}
\mathbf{X} &= [\mathbf{x}(0), \mathbf{x}(1), \cdots, \mathbf{x}(N-1)], \\
\mathbf{S}_D(\mathbf{f}_D) &= [\mathbf{s}_D(\mathbf{f}_D, 0), \mathbf{s}_D(\mathbf{f}_D, 1), \cdots, \mathbf{s}_D(\mathbf{f}_D, N-1)], \\
\mathbf{S}(\boldsymbol{\tau}) &= [\mathbf{s}_{\boldsymbol{\tau}}(0), \mathbf{s}_{\boldsymbol{\tau}}(1), \cdots, \mathbf{s}_{\boldsymbol{\tau}}(N-1)], \\
\mathbf{W} &= [\mathbf{w}(0), \mathbf{w}(1), \cdots, \mathbf{w}(N-1)].
\end{aligned} \tag{5}$$

Similar to [23, 24], it is assumed that the additive noises are temporally and spatially white with zero-mean and variance σ_w^2, and are uncorrelated with the incident signals.

3. Proposed Method

3.1. Nonlinear Least Squares Based ML method

Similar to [13], we can formulate a maximum likelihood (ML) cost function as follows,

$$\{\hat{\boldsymbol{\theta}}, \hat{\boldsymbol{\tau}}, \hat{\mathbf{f}}_D, \hat{\boldsymbol{\gamma}}\} = \arg\min_{\boldsymbol{\theta},\boldsymbol{\tau},\mathbf{f}_D,\boldsymbol{\gamma}} ||\mathbf{X} - \mathbf{B}(\boldsymbol{\theta}, \boldsymbol{\gamma})(\mathbf{S}_D(\mathbf{f}_D) \circ \mathbf{S}(\boldsymbol{\tau}))||_F^2 \tag{6}$$

Using the projection theory, the estimations of $\boldsymbol{\theta}, \boldsymbol{\tau}, \mathbf{f}_D$, and $\boldsymbol{\gamma}$ can be separated, i.e., (6) can be transformed into

$$\{\hat{\boldsymbol{\tau}}, \hat{\mathbf{f}}_D\} = \arg\min_{\boldsymbol{\tau},\mathbf{f}_D} \left\|\mathbf{P}^{\perp}_{\mathbf{S}_D^T(\mathbf{f}_D)\circ\mathbf{S}^T(\boldsymbol{\tau})}\mathbf{X}^T\right\|_F^2 \tag{7}$$

$$\hat{\mathbf{B}}(\hat{\boldsymbol{\theta}}, \hat{\boldsymbol{\gamma}}) = \mathbf{X}(\mathbf{S}_D(\hat{\mathbf{f}}_D) \circ \mathbf{S}(\hat{\boldsymbol{\tau}}))^{\dagger} \tag{8}$$

where $\mathbf{P}_{\mathbf{S}_D^T(\mathbf{f}_D)\circ\mathbf{S}^T(\boldsymbol{\tau})} = (\mathbf{S}_D^T(\mathbf{f}_D)\circ\mathbf{S}^T(\boldsymbol{\tau}))(\mathbf{S}_D^T(\mathbf{f}_D) \circ \mathbf{S}^T(\boldsymbol{\tau}))^{\dagger}$, and $\mathbf{P}^{\perp}_{\mathbf{S}_D^T(\mathbf{f}_D)\circ\mathbf{S}^T(\boldsymbol{\tau})} = \mathbf{I}_N - \mathbf{P}_{\mathbf{S}_D^T(\mathbf{f}_D)\circ\mathbf{S}^T(\boldsymbol{\tau})}$ represent the projection and orthogonal projection matrices of $\mathbf{S}_D^T(\mathbf{f}_D) \circ \mathbf{S}^T(\boldsymbol{\tau})$, respectively.

With the aid of the vectorization operator, the cost function in (7) can be expressed as

$$\begin{aligned}
&||\mathbf{P}^{\perp}_{\mathbf{S}_D^T(\mathbf{f}_D)\circ\mathbf{S}^T(\boldsymbol{\tau})}\mathbf{X}^T||_F^2 \\
&= ||\mathrm{vec}\{\mathbf{P}^{\perp}_{\mathbf{S}_D^T(\mathbf{f}_D)\circ\mathbf{S}^T(\boldsymbol{\tau})}\mathbf{X}^T\}||_2^2 \\
&= ||\mathrm{vec}\{\mathbf{X}^T\} - (\mathbf{X} \otimes \mathbf{I}_N) \cdot \mathrm{vec}\{\mathbf{P}_{\mathbf{S}_D^T(\mathbf{f}_D)\circ\mathbf{S}^T(\boldsymbol{\tau})}\}||_2^2
\end{aligned} \tag{9}$$

It is noticed that time delays and Doppler shifts are nonlinearly mixed with known waveforms, and we now have a nonlinear least squares (NLS) problem, which can be solved via the Levenberg-Marquardt algorithm [25]. Therefore, we can obtain estimates of $\boldsymbol{\tau}$ and $\mathbf{f}_D$ via NLS optimization, provided a good initialization is available.

With the estimates of time delays and Doppler shifts and (8), DOA and complex amplitude can be estimated as follows

$$\hat{\theta}_q = \arcsin\{\frac{-\lambda}{2\pi d} \cdot \text{angle}\{\frac{1}{M-1}\sum_{m=1}^{M-1}\frac{\hat{\mathbf{B}}_{m+1,q}}{\hat{\mathbf{B}}_{m,q}}\}\} \tag{10}$$

$$\hat{\gamma}_q = \frac{1}{M}\sum_{m=1}^{M}\frac{\hat{\mathbf{B}}_{m,q}}{\exp\{-j2\pi(m-1)d\sin\hat{\theta}_q/\lambda\}} \tag{11}$$

where $\hat{\mathbf{B}}_{m,q}$ denotes the (m,q)th element of $\hat{\mathbf{B}}(\hat{\boldsymbol{\theta}}, \hat{\boldsymbol{\gamma}})$.

3.2. Initialization with the Toeplitz Dominant Rule

To provide good initial estimates, we can find a solution to reduce the optimization dimension of (7).

Utilizing the property of matrix trace, (7) can be rewritten as

$$\begin{aligned}
\{\hat{\boldsymbol{\tau}}, \hat{\mathbf{f}}_D\} &= \arg\min_{\boldsymbol{\tau},\mathbf{f}_D} \left\|\mathbf{P}^{\perp}_{\mathbf{S}_D^T(\mathbf{f}_D)\circ\mathbf{S}^T(\boldsymbol{\tau})}\mathbf{X}^T\right\|_F^2 \\
&= \arg\min_{\boldsymbol{\tau},\mathbf{f}_D} \text{tr}\{\mathbf{X}^*(\mathbf{P}^{\perp}_{\mathbf{S}_D^T(\mathbf{f}_D)\circ\mathbf{S}^T(\boldsymbol{\tau})})^H\mathbf{P}^{\perp}_{\mathbf{S}_D^T(\mathbf{f}_D)\circ\mathbf{S}^T(\boldsymbol{\tau})}\mathbf{X}^T\} \\
&= \arg\min_{\boldsymbol{\tau},\mathbf{f}_D} \text{tr}\{\mathbf{X}^*\mathbf{P}^{\perp}_{\mathbf{S}_D^T(\mathbf{f}_D)\circ\mathbf{S}^T(\boldsymbol{\tau})}\mathbf{X}^T\} \\
&= \arg\min_{\boldsymbol{\tau},\mathbf{f}_D} \text{tr}\{\mathbf{X}^T\mathbf{X}^*\mathbf{P}^{\perp}_{\mathbf{S}_D^T(\mathbf{f}_D)\circ\mathbf{S}^T(\boldsymbol{\tau})}\} \\
&= \arg\min_{\boldsymbol{\tau},\mathbf{f}_D} \text{tr}\{\mathbf{X}^T\mathbf{X}^*\} - \text{tr}\{\mathbf{X}^T\mathbf{X}^*\mathbf{P}_{\mathbf{S}_D^T(\mathbf{f}_D)\circ\mathbf{S}^T(\boldsymbol{\tau})}\} \\
&= \arg\max_{\boldsymbol{\tau},\mathbf{f}_D}\ \text{tr}\{\mathbf{X}^T\mathbf{X}^*\mathbf{P}_{\mathbf{S}_D^T(\mathbf{f}_D)\circ\mathbf{S}^T(\boldsymbol{\tau})}\} \\
&= \arg\max_{\boldsymbol{\tau},\mathbf{f}_D}\ \text{tr}\{\mathbf{X}^H\mathbf{X}\mathbf{P}_{\mathbf{S}_D^H(\mathbf{f}_D)\circ\mathbf{S}^H(\boldsymbol{\tau})}\}
\end{aligned} \tag{12}$$

For a large number of snapshots N, we have the following approximation

$$\begin{aligned}&(\mathbf{S}_D(\mathbf{f}_D)\circ\mathbf{S}(\tau))(\mathbf{S}_D^H(\mathbf{f}_D)\circ\mathbf{S}^H(\tau))\\ \approx&\text{diag}\{(\mathbf{s}_1(f_{D1})\circ\mathbf{s}_1(\tau_1))(\mathbf{s}_1^H(f_{D1})\circ\mathbf{s}_1^H(\tau_1)),\cdots,\\ &(\mathbf{s}_Q(f_{DQ})\circ\mathbf{s}_Q(\tau_Q))(\mathbf{s}_Q^H(f_{DQ})\circ\mathbf{s}_Q^H(\tau_Q))\}\end{aligned}\tag{13}$$

where $\mathbf{s}_q(\tau_q)=[s_q(0-\tau_q),s_q(1-\tau_q),\cdots,s_q(N-1-\tau_q)]$, $\mathbf{s}_q(f_{Dq})=[1,e^{j2\pi f_{Dq}},\cdots,e^{j2\pi f_{Dq}(N-1)}]$, and $q=1,\cdots,Q$.

Substituting (13) into (12), we have

$$\begin{aligned}&\text{tr}\{\mathbf{X}^H\mathbf{X}\mathbf{P}_{\mathbf{S}_D^H(\mathbf{f}_D)\circ\mathbf{S}^H(\boldsymbol{\tau})}\}\\ =&\text{tr}\{\mathbf{X}^H\mathbf{X}(\mathbf{S}_D^H(\mathbf{f}_D)\circ\mathbf{S}^H(\boldsymbol{\tau}))(\mathbf{S}_D^H(\mathbf{f}_D)\circ\mathbf{S}^H(\boldsymbol{\tau}))^\dagger\}\\ =&\text{tr}\{\mathbf{X}^H\mathbf{X}(\mathbf{S}_D^H(\mathbf{f}_D)\circ\mathbf{S}^H(\boldsymbol{\tau}))((\mathbf{S}_D(\mathbf{f}_D)\circ\mathbf{S}(\boldsymbol{\tau}))(\mathbf{S}_D^H(\mathbf{f}_D)\circ\mathbf{S}^H(\boldsymbol{\tau})))^{-1}(\mathbf{S}_D(\mathbf{f}_D)\circ\mathbf{S}(\boldsymbol{\tau}))\}\\ \approx&\sum_{q=1}^{Q}\frac{(\mathbf{s}_q(f_{Dq})\circ\mathbf{s}_q(\tau_q))\mathbf{X}^H\mathbf{X}(\mathbf{s}_q^H(f_{Dq})\circ\mathbf{s}_q^H(\tau_q))}{(\mathbf{s}_q(f_{Dq})\circ\mathbf{s}_q(\tau_q))(\mathbf{s}_q^H(f_{Dq})\circ\mathbf{s}_q^H(\tau_q))}\end{aligned}\tag{14}$$

Hence, time delays and Doppler shifts can be estimated using Q two-dimensional (2-D) searches as follows,

$$\{\hat{\tau}_q,\hat{f}_{Dq}\}=\arg\max_{\tau,f_D}\frac{(\mathbf{s}_q(f_D)\circ\mathbf{s}_q(\tau))\mathbf{X}^H\mathbf{X}(\mathbf{s}_q^H(f_D)\circ\mathbf{s}_q^H(\tau))}{(\mathbf{s}_q(f_D)\circ\mathbf{s}_q(\tau))(\mathbf{s}_q^H(f_D)\circ\mathbf{s}_q^H(\tau))}\tag{15}$$

Using the property of Hadamard product, (15) can be rewritten as

$$\{\hat{\tau}_q,\hat{f}_{Dq}\}=\arg\max_{\tau,f_D}\frac{\mathbf{s}_q(f_D)\text{diag}\{\mathbf{s}_q(\tau)\}\mathbf{X}^H\mathbf{X}\text{diag}\{\mathbf{s}_q^H(\tau)\}\mathbf{s}_q^H(f_D)}{\mathbf{s}_q(\tau)\mathbf{s}_q^H(\tau)}\tag{16}$$

However, the 2-D search of (16) still has a high computational complexity. To reduce it further, notice that

$$\begin{aligned}\mathbf{X}^H\mathbf{X}=&M\sum_{q=1}^{Q}|\gamma_q|^2\mathbf{s}_{qq}^H(f_{Dq},\tau_q)\mathbf{s}_{qq}(f_{Dq},\tau_q)\\ &+\sum_{r=1}^{Q}\sum_{p=1,p\neq r}^{Q}\gamma_r^*\gamma_p\mathbf{s}_{rr}^H(f_{Dr},\tau_r)\mathbf{a}^H(\theta_r)\mathbf{a}(\theta_p)\mathbf{s}_{pp}(f_{Dp},\tau_p)+\mathbf{E}\end{aligned}\tag{17}$$

where $\mathbf{s}_{qr}(f_{Dq}, \tau_r) = \mathbf{s}_q(f_{Dq}) \circ \mathbf{s}_r(\tau_r)$, and $\mathbf{E} = \mathbf{W}^H \mathbf{B}(\boldsymbol{\theta}, \boldsymbol{\gamma}) \cdot (\mathbf{S}_D(\mathbf{f}_D) \circ \mathbf{S}(\tau)) + (\mathbf{S}_D(\mathbf{f}_D) \circ \mathbf{S}(\tau))^H \mathbf{B}^H(\boldsymbol{\theta}, \boldsymbol{\gamma}) \mathbf{W} + \mathbf{W}^H \mathbf{W}$.

Hence, if $\tau = \tau_q$, we have

$$\begin{aligned} &\mathrm{diag}^{-1}\{\mathbf{s}_{qq}(\tau_q, \tau_q)\}\mathrm{diag}\{\mathbf{s}_q(\tau_q)\}\mathbf{X}^H\mathbf{X} \cdot \mathrm{diag}\{\mathbf{s}_q^H(\tau_q)\}\mathrm{diag}^{-1}\{\mathbf{s}_{qq}(\tau_q, \tau_q)\} \\ &= \mathbf{C}_0 + \mathbf{C}_1 + \mathbf{C}_2 + \mathbf{C}_3 \end{aligned} \tag{18}$$

where

$$\mathbf{C}_0 = M|\gamma_q|^2 \mathbf{s}_q^H(f_{D_q})\mathbf{s}_q(f_{Dq}) \tag{19}$$

$$\begin{aligned} \mathbf{C}_1 = &M \sum_{p=1, p\neq q}^{Q} |\gamma_p|^2 \mathrm{diag}^{-1}\{\mathbf{s}_{qq}(\tau_q, \tau_q)\} \\ &\cdot \mathrm{diag}\{\mathbf{s}_{qp}(\tau_q, \tau_p)\}\mathbf{s}_p^H(f_{D_p})\mathbf{s}_p(f_{Dp})\mathrm{diag}\{\mathbf{s}_{pq}(\tau_p, \tau_q)\} \cdot \mathrm{diag}^{-1}\{\mathbf{s}_{qq}(\tau_q, \tau_q)\} \end{aligned} \tag{20}$$

$$\begin{aligned} \mathbf{C}_2 = &\sum_{r=1}^{Q} \sum_{p=1, p\neq r}^{Q} \gamma_t^* \gamma_p \mathrm{diag}^{-1}\{\mathbf{s}_{qq}(\tau_q, \tau_q)\} \cdot \mathrm{diag}\{\mathbf{s}_{qr}(\tau_q, \tau_r)\}\mathbf{s}_r^H(f_{D_r})\mathbf{a}^H(\theta_r)\mathbf{a}(\theta_p)\mathbf{s}_p(f_{Dp}) \\ &\cdot \mathrm{diag}\{\mathbf{s}_{pq}(\tau_p, \tau_q)\}\mathrm{diag}^{-1}\{\mathbf{s}_{qq}(\tau_q, \tau_q)\} \end{aligned} \tag{21}$$

$$\mathbf{C}_3 = \mathrm{diag}\{\mathbf{s}_q(\tau_q)\}\mathbf{E}\mathrm{diag}\{\mathbf{s}_q^H(\tau_q)\} \tag{22}$$

$$\mathrm{diag}\{\mathbf{s}_{qr}(\tau_q, \tau_r)\} = \mathrm{diag}\{\mathbf{s}_q(\tau_q) \circ \mathbf{s}_r^*(\tau_r)\} \tag{23}$$

Since $\mathbf{C}_0$ is a Toeplitz matrix, while $\mathbf{C}_1$, $\mathbf{C}_2$, and $\mathbf{C}_3$ are not, we can establish a Toeplitz dominant rule to determine the time delay without known Doppler shift as follows,

$$\hat{\tau}_q = \arg\min_{\tau} ||\mathbf{G}_q(\tau) - \mathrm{Toeplitz}\{\mathbf{g}_{q,1}(\tau)\}||_F^2 \tag{24}$$

where

$$\begin{aligned} \mathbf{G}_q(\tau) = &\mathrm{diag}^{-1}\{\mathbf{s}_{qq}(\tau, \tau)\}\mathrm{diag}\{\mathbf{s}_q(\tau)\}\mathbf{X}^H\mathbf{X} \\ &\cdot \mathrm{diag}\{\mathbf{s}_q^H(\tau)\}\mathrm{diag}^{-1}\{\mathbf{s}_{qq}(\tau, \tau)\}, \end{aligned} \tag{25}$$

$\mathbf{g}_{q,1}(\tau)$ is the first row of $\mathbf{G}_q(\tau)$, and Toeplitz$\{\cdot\}$ denotes Toeplitz matrix construction using a row vector.

Furthermore, to improve the time delay estimation performance under low SNR cases, a multiple frame superposition strategy is adopted. To start, $\mathbf{X}$ and $\mathbf{s}_q(\tau)$ are divided into L frames with maximum overlap along the snapshot dimension, i.e., $\mathbf{X}^{(l)} = \mathbf{X}_{:,l:l+N-L}$, $\mathbf{s}_q^{(l)}(\tau) = \mathbf{s}_{q,l:l+N-L}(\tau)$, $l = 0, 1, \cdots, L-1$. Then, the cost function of (24) is applied L times, and a summation of these results leads to a new estimate of the time delay.

Substituting the estimates of $\{\hat{\tau}_q\}_{q=1}^{Q}$ into (16), we can obtain the estimates of Doppler shifts $\{\hat{f}_{D_q}\}_{q=1}^{Q}$ via Q 1-D searches. Moreover, higher-accuracy estimates of time delays and Doppler shifts can be obtained by applying the NLS optimization method to (9).

Remark 1: For the initial estimates of time delays and Doppler shifts in (16) and (24), we can utilize some simple search strategy such as in [6], to reduce the number of searches.

3.3. Summary of the proposed method

The steps of the proposed method are summarized as follows:

Step 1: Divide $\mathbf{X}$ and $\mathbf{s}_q(\tau)$ into L frames with maximum overlap along the snapshot dimension, i.e., $\mathbf{X}^{(l)} = \mathbf{X}_{:,l:l+N-L}$, $\mathbf{s}_q^{(l)}(\tau) = \mathbf{s}_{q,l:l+N-L}(\tau)$, $\mathbf{s}_q^{(l)}(f_{D_q}) = \mathbf{s}_{q,l:l+N-L}(f_{D_q})$, $l = 0, 1, \cdots, L-1$.

Step 2: With $\mathbf{X}^{(l)}$ and $\{\mathbf{s}_q^{(l)}(\tau)\}_{q=1}^{Q}$ and using cost function of (24) QL times, obtain the initial estimates of time delays , i.e., $\{\hat{\tau}_q\}_{q=1}^{Q}$.

Step 3: Applying Q 1-D searches to (16) with $\{\hat{\tau}_q\}_{q=1}^{Q}$, get the initial estimates of Doppler shifts $\{\hat{f}_{D_q}\}_{q=1}^{Q}$.

Step 4: With the aid of $\{\hat{\tau}_q\}_{q=1}^{Q}$ and $\{\hat{f}_{D_q}\}_{q=1}^{Q}$, obtain the high accuracy estimates of $\boldsymbol{\tau}$ and $\mathbf{f}_D$ from (7) and (9) via NLS optimization[1].

Step 5: Obtain the estimates of DOAs and complex amplitudes from (8), (10), and (11).

3.4. Computational complexity analysis

In this subsection, the computational complexity of the proposed method is compared with those of DEML[12], Swindlehurst [13], and OP[24]. However, please note that they work on different conditions as shown in Tab. 1 and only the proposed method can work on the most general scenario.

Table 1: Required conditions of the four methods.

	Proposed	DEML	Swindlehurst	OP
Time delay	Unknown	Known	Unknown	Known
Doppler shift	Unknown	Known	Known	Unknown

For the proposed method (the following analysis is consistent with steps in Section 3.4):

(i) Initial estimates of $\{\hat{\tau}_q\}_{q=1}^{Q}$: $O\{MN^2+Q(N-L+1)^2NL+QN_\tau L(N-L+1)\}$, where N_τ denotes the number of time delay searches.

(ii) Initial estimates of $\{\hat{f}_{D_q}\}_{q=1}^{Q}$: $O\{QN_{f_D}N^2\}$, where N_{f_D} denotes the number of Doppler shift searches.

(iii) NLS based high accuracy estimates of $\boldsymbol{\tau}$ and $\mathbf{f}_D$: $O\{N_{iter}(2Q)^2MN+N_{iter}(2Q)^3\}$, where N_{iter} denotes the number of iterations.

[1] One can use the MATLAB function *lsqnonlin* to realize the Levenberg-Marquardt algorithm.

(iv) DOA and complex amplitude estimation: $O\{Q^2N + MNQ + 2Q + 2QM\}$.

Then, with $N_\tau \approx N_{f_D} \approx N > L \approx M > Q$ and N_{iter} being less than 20 in practice, the overall computational complexity of the proposed method is approximately $O\{MN^2 + QN_\tau NL + QN_{f_D}N^2 + 4N_{iter}MNQ\}$.

For the DEML method, its overall computational complexity is about $O\{M^2N + MQN + 3M^3\}$ [23].

Considering the Swindlehurst method, where the high accuracy time delay estimates also utilize the NLS optimization, its computational complexity is approximately $O\{MN^2 + QN_\tau N^2 + N_{iter}MNQ\}$, which is similar to that of the proposed method.

In terms of the OP method, its overall computational complexity is about $O\{MN\log_2 N + (P+1)N^3 + (P+1)(P+2)QN^2 + (P+1)QMN\}$ [24].

It can be seen that the proposed method has a larger computational complexity than the other three methods owing to the multiple 1-D searches involved in the initial estimates of time delays and Doppler shifts. However, its computational complexity is still less than the direct 2-D search based optimization of (7) and subsequent DOA and complex amplitude estimation.

4. Simulation Results

In this section, the performance of the proposed method is compared with those of DEML[12], Swindlehurst [13], and OP[24], and the Cramer-Rao bound (CRB) for unknown waveforms [26], and known waveforms with unknown time delays and Doppler shifts (similar to [24], see Appendix for details), respectively, according to their own working conditions as listed in

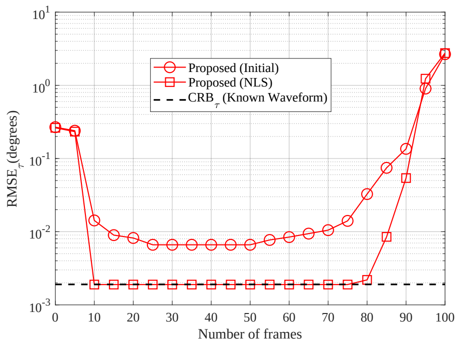

(a) Time delay

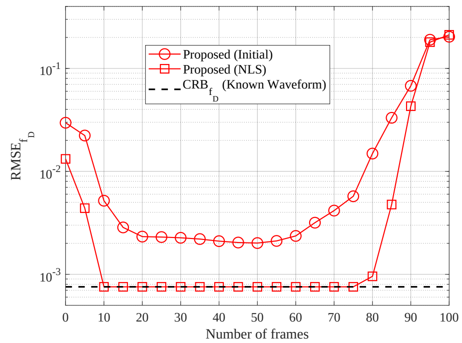

(b) Doppler shift

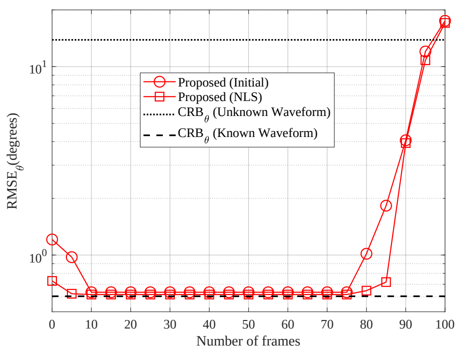

(c) DOA

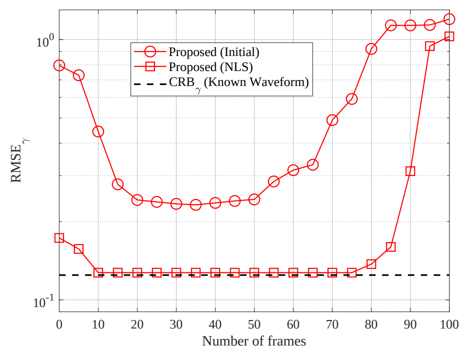

(d) Complex amplitude

Figure 1: RMSE versus number of frames, $K = 3$, $M = 4$, $N = 100$, SNR=0 dB.

Tab. 1. It is assumed that $d = \lambda/2$, and the waveforms of all sources are known with unit power. However, please bear in mind that these methods work on different conditions and only the proposed one works on the most general scenario where all the others fail. So their performances are not directly comparable and the reason to show their performances together here is to give some idea of the performance of the proposed method in the context of the class of algorithms available to deal with known waveforms but with different unknown conditions.

Example 1: In the first example, the performance of the proposed method

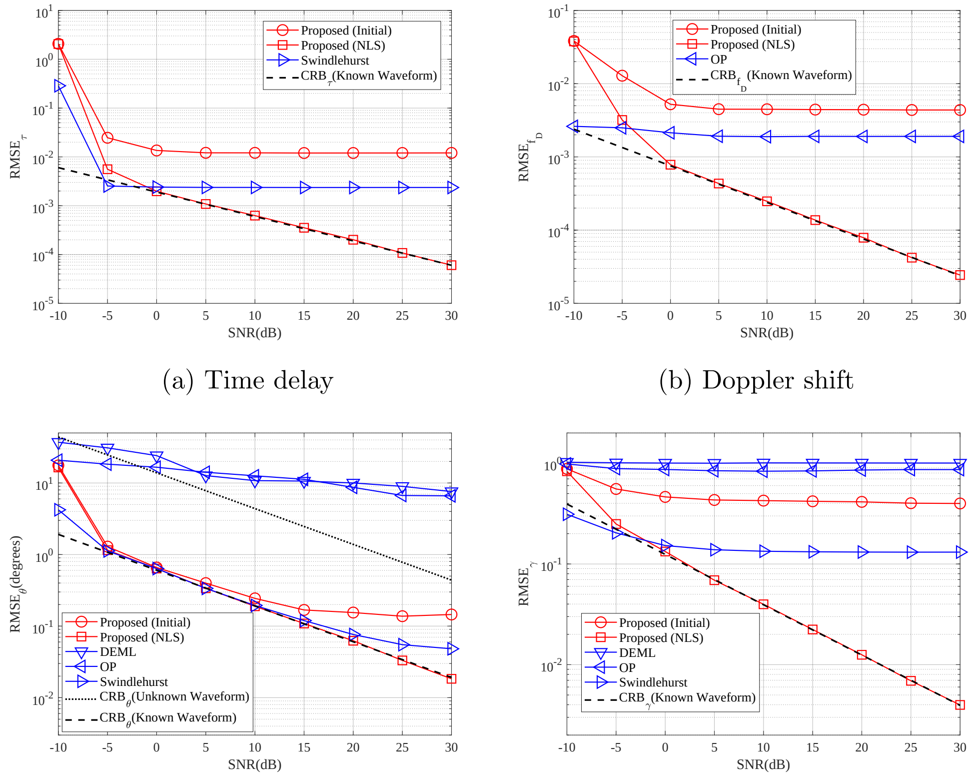

(a) Time delay

(b) Doppler shift

(c) DOA

(d) Complex amplitude

Figure 2: RMSE versus SNR, $K = 3$, $M = 4$, $N = 100$, L=10.

with respect to the number of frames L is studied. The time delays, Doppler shifts, DOAs, and complex amplitudes of three sources are set to 2.4, 3.6, 1.3, 10^{-3}, 10^{-3}, 10^{-3}, $-10°$, $10°$, $15°$, $e^{j0.3\pi}$, $e^{-j0.4\pi}$, and $e^{-j0.2\pi}$, respectively. With $M = 4$ and SNR = 10 dB, L varies from 0 to 100 with an interval of 5. The root mean square error (RMSE) results based on 500 Monte Carlo trials for each fixed L are shown in Fig. 1.

It can be seen that the performance of NLS method largely depends on the initial estimates, and a modest number of frames can provide sufficient

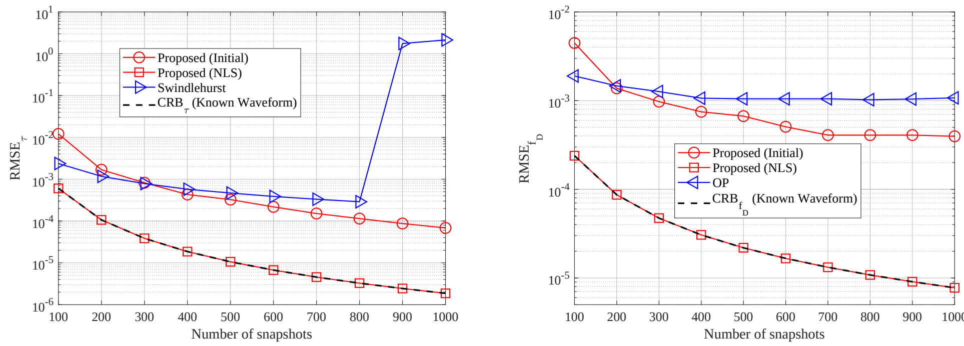

(a) Time delay (b) Doppler shift

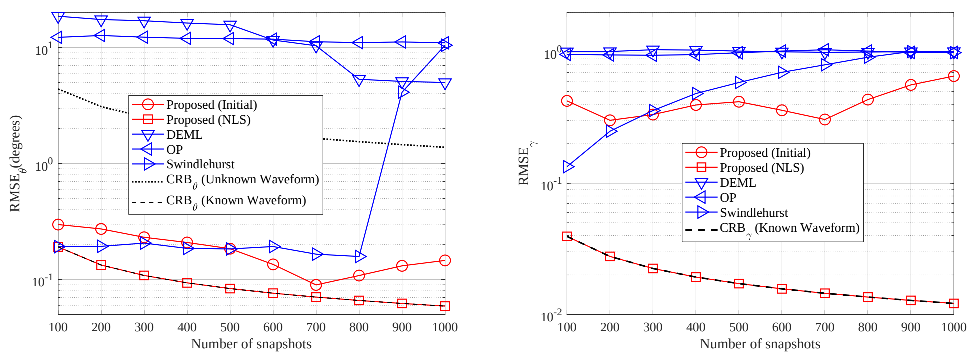

(c) DOA (d) Complex amplitude

Figure 3: RMSE versus number of snapshots, $K = 3$, $M = 4$, SNR = 10dB, $L = 10$.

estimation accuracy. Besides, since (13)-(15) are derived from the approximation for a large number of snapshots, there is a gap between the estimation performance of Toeplitz dominant rule based initialization method and the NLS method.

Examples 2 & 3: In Example 2, we investigate the performance of the proposed method with respect to SNR. The settings are the same as in Example 1 except that $L = 10$, and SNR varies from -10dB to 30dB with an interval of 5dB. The results are provided in Fig. 2. In Example 3, the performance of the proposed method against the number of snapshots is examined. The settings are the same as in Example 2 except that SNR = 10 dB and N ranges from 100 to 1000 with an interval of 100. Fig. 3 shows the results.

As shown in Figs. 2 and 3, the proposed NLS based method can work effectively for ranges of SNR from 0dB to 30dB and N from 100 to 1000. Moreover, its performance outperforms the other four methods and can approach the CRB for high SNR values and a large number of snapshots. The good performance of the proposed method is mainly due to employment of the nonlinear least squares optimization by making effective use of the structural information of signal model in the presence of unknown time delays and Doppler shifts.

For the proposed Toeplitz dominant rule based initialization method, as seen from Fig. 2, its performance cannot be improved with increasing SNR since it is mainly related to the approximation error of (13). Moreover, as shown in Fig. 3, there are some unstable estimation performances of DOA and complex amplitude, which may be due to that the correlation of source signals varies with the number of snapshots and similar results have been observed in [13].

From Figs. 2 and 3, for the OP method proposed earlier in [24], it cannot work well for most cases since its performance is sensitive to model bias. While the Swindlehurst's method in [13] is derived from the ML principle and has shown more robustness against the bias of model, since it does not consider the Doppler effect, it can not work effectively for a large number of snapshots.

5. Conclusions

A novel DOA estimation method for sources with known waveforms in the presence of unknown time delays and Doppler shifts has been introduced. Based on the maximum likelihood idea and the matrix projection theory, a decoupled cost function was first established and then the estimation of time delay and Doppler shift was transformed into a nonlinear least squares (NLS) problem. To solve the NLS problem efficiently, a Toeplitz dominant rule was employed to provide initial estimates with a reduced dimension; finally, with the aid of time delay and Doppler estimates, the DOAs and complex amplitudes were obtained based on the data structure information. As demonstrated by computer simulations, the proposed method can achieve a performance close to CRB for the high SNR and larger number of snapshot case in the presence of unknown time delays and Doppler shifts.

Appendix : Derivation of the CRB

Similar to [24], the vector consisting of all real-valued unknown variables of the model in (4) can be expressed as

$$\boldsymbol{\mu} = [\boldsymbol{\theta}^T, \boldsymbol{\xi}^T, \boldsymbol{\eta}^T, \boldsymbol{\tau}^T, \mathbf{f}_D^T]^T \tag{26}$$

where $\boldsymbol{\xi} = [\xi_1, \cdots, \xi_Q]^T = [\mathrm{Re}(\gamma_1), \cdots, \mathrm{Re}(\gamma_Q)]^T$, $\boldsymbol{\eta} = [\xi_1, \cdots, \xi_Q]^T = [\mathrm{Im}(\gamma_1), \cdots, \mathrm{Im}(\gamma_Q)]^T$.

For simplicity, $\mathbf{A}(\boldsymbol{\theta})$ and $\boldsymbol{\Gamma}(\boldsymbol{\gamma})$ are denoted as $\mathbf{A}$ and $\boldsymbol{\Gamma}$. Besides, $\widehat{\mathbf{s}}(n) = \mathbf{s}_D(\mathbf{f}_D, n) \circ \mathbf{s}_\tau(n)$, and $\mathbf{x}_0(n) = \mathbf{A}\boldsymbol{\Gamma}\widehat{\mathbf{s}}(n)$.

Similar to [24, 27], the corresponding Fisher information matrix can be expressed as follows,

$$\mathbf{I}(\boldsymbol{\mu}) = \frac{2}{\sigma_w^2}\mathrm{Re}\left(\begin{bmatrix} \mathbf{I}_{\boldsymbol{\theta}\boldsymbol{\theta}} & \mathbf{I}_{\boldsymbol{\theta}\boldsymbol{\xi}} & \mathbf{I}_{\boldsymbol{\theta}\boldsymbol{\eta}} & \mathbf{I}_{\boldsymbol{\theta}\boldsymbol{\tau}} & \mathbf{I}_{\boldsymbol{\theta}\mathbf{f}_D} \\ \mathbf{I}_{\boldsymbol{\xi}\boldsymbol{\theta}} & \mathbf{I}_{\boldsymbol{\xi}\boldsymbol{\xi}} & \mathbf{I}_{\boldsymbol{\xi}\boldsymbol{\eta}} & \mathbf{I}_{\boldsymbol{\xi}\boldsymbol{\tau}} & \mathbf{I}_{\boldsymbol{\xi}\mathbf{f}_D} \\ \mathbf{I}_{\boldsymbol{\eta}\boldsymbol{\theta}} & \mathbf{I}_{\boldsymbol{\eta}\boldsymbol{\xi}} & \mathbf{I}_{\boldsymbol{\eta}\boldsymbol{\eta}} & \mathbf{I}_{\boldsymbol{\eta}\boldsymbol{\tau}} & \mathbf{I}_{\boldsymbol{\eta}\mathbf{f}_D} \\ \mathbf{I}_{\boldsymbol{\tau}\boldsymbol{\theta}} & \mathbf{I}_{\boldsymbol{\tau}\boldsymbol{\xi}} & \mathbf{I}_{\boldsymbol{\tau}\boldsymbol{\eta}} & \mathbf{I}_{\boldsymbol{\tau}\boldsymbol{\tau}} & \mathbf{I}_{\boldsymbol{\tau}\mathbf{f}_D} \\ \mathbf{I}_{\mathbf{f}_D\boldsymbol{\theta}} & \mathbf{I}_{\mathbf{f}_D\boldsymbol{\xi}} & \mathbf{I}_{\mathbf{f}_D\boldsymbol{\eta}} & \mathbf{I}_{\mathbf{f}_D\boldsymbol{\tau}} & \mathbf{I}_{\mathbf{f}_D\mathbf{f}_D} \end{bmatrix}\right) \tag{27}$$

where

$$\mathbf{I}_{\boldsymbol{\theta}\boldsymbol{\theta}} = N \cdot (\boldsymbol{\Gamma}^H \dot{\mathbf{A}}^H \dot{\mathbf{A}} \boldsymbol{\Gamma}) \circ \mathbf{R}^T_{\overset{\frown}{s}\overset{\frown}{s}} \tag{28}$$

$$\mathbf{I}_{\boldsymbol{\theta}\boldsymbol{\xi}} = \mathbf{I}^H_{\boldsymbol{\xi}\boldsymbol{\theta}} = N \cdot (\boldsymbol{\Gamma}^H \dot{\mathbf{A}}^H \mathbf{A} \dot{\boldsymbol{\Gamma}}_\xi) \circ \mathbf{R}^T_{\overset{\frown}{s}\overset{\frown}{s}} \tag{29}$$

$$\mathbf{I}_{\boldsymbol{\theta}\boldsymbol{\eta}} = \mathbf{I}^H_{\boldsymbol{\eta}\boldsymbol{\theta}} = N \cdot (\boldsymbol{\Gamma}^H \dot{\mathbf{A}}^H \mathbf{A} \dot{\boldsymbol{\Gamma}}_\eta) \circ \mathbf{R}^T_{\overset{\frown}{s}\overset{\frown}{s}} \tag{30}$$

$$\mathbf{I}_{\boldsymbol{\theta}\boldsymbol{\tau}} = \mathbf{I}^H_{\boldsymbol{\tau}\boldsymbol{\theta}} = N \cdot (\boldsymbol{\Gamma}^H \dot{\mathbf{A}}^H \mathbf{A} \boldsymbol{\Gamma}) \circ \mathbf{R}^T_{\tilde{s}\overset{\frown}{s}} \tag{31}$$

$$\mathbf{I}_{\boldsymbol{\theta}\mathbf{f}_D} = \mathbf{I}^H_{\mathbf{f}_D\boldsymbol{\theta}} = N \cdot (\boldsymbol{\Gamma}^H \dot{\mathbf{A}}^H \mathbf{A} \boldsymbol{\Gamma}) \circ \mathbf{R}^T_{\overset{\smile}{s}\overset{\frown}{s}} \tag{32}$$

$$\mathbf{I}_{\boldsymbol{\xi}\boldsymbol{\xi}} = N \cdot (\dot{\boldsymbol{\Gamma}}^H_\xi \mathbf{A}^H \mathbf{A} \dot{\boldsymbol{\Gamma}}_\xi) \circ \mathbf{R}^T_{\overset{\frown}{s}\overset{\frown}{s}} \tag{33}$$

$$\mathbf{I}_{\boldsymbol{\xi}\boldsymbol{\eta}} = \mathbf{I}^H_{\boldsymbol{\eta}\boldsymbol{\xi}} = N \cdot (\dot{\boldsymbol{\Gamma}}^H_\xi \mathbf{A}^H \mathbf{A} \dot{\boldsymbol{\Gamma}}_\eta) \circ \mathbf{R}^T_{\overset{\frown}{s}\overset{\frown}{s}} \tag{34}$$

$$\mathbf{I}_{\boldsymbol{\xi}\boldsymbol{\tau}} = \mathbf{I}^H_{\boldsymbol{\tau}\boldsymbol{\xi}} = N \cdot (\dot{\boldsymbol{\Gamma}}^H_\xi \mathbf{A}^H \mathbf{A} \boldsymbol{\Gamma}) \circ \mathbf{R}^T_{\tilde{s}\overset{\frown}{s}} \tag{35}$$

$$\mathbf{I}_{\boldsymbol{\xi}\mathbf{f}_D} = \mathbf{I}^H_{\mathbf{f}_D\boldsymbol{\xi}} = N \cdot (\dot{\boldsymbol{\Gamma}}^H_\xi \mathbf{A}^H \mathbf{A} \boldsymbol{\Gamma}) \circ \mathbf{R}^T_{\overset{\smile}{s}\overset{\frown}{s}} \tag{36}$$

$$\mathbf{I}_{\boldsymbol{\eta}\boldsymbol{\eta}} = N \cdot (\dot{\boldsymbol{\Gamma}}^H_\eta \mathbf{A}^H \mathbf{A} \dot{\boldsymbol{\Gamma}}_\eta) \circ \mathbf{R}^T_{\overset{\frown}{s}\overset{\frown}{s}} \tag{37}$$

$$\mathbf{I}_{\boldsymbol{\eta}\boldsymbol{\tau}} = \mathbf{I}^H_{\boldsymbol{\tau}\boldsymbol{\eta}} = N \cdot (\dot{\boldsymbol{\Gamma}}^H_\eta \mathbf{A}^H \mathbf{A} \boldsymbol{\Gamma}) \circ \mathbf{R}^T_{\tilde{s}\overset{\frown}{s}} \tag{38}$$

$$\mathbf{I}_{\boldsymbol{\eta}\mathbf{f}_D} = \mathbf{I}^H_{\mathbf{f}_D\boldsymbol{\eta}} = N \cdot (\dot{\boldsymbol{\Gamma}}^H_\eta \mathbf{A}^H \mathbf{A} \boldsymbol{\Gamma}) \circ \mathbf{R}^T_{\overset{\smile}{s}\overset{\frown}{s}} \tag{39}$$

$$\mathbf{I}_{\boldsymbol{\tau}\boldsymbol{\tau}} = N \cdot (\boldsymbol{\Gamma}^H \mathbf{A}^H \mathbf{A} \boldsymbol{\Gamma}) \circ \mathbf{R}^T_{\tilde{s}\tilde{s}} \tag{40}$$

$$\mathbf{I}_{\boldsymbol{\tau}\mathbf{f}_D} = \mathbf{I}^H_{\mathbf{f}_D\boldsymbol{\tau}} = N \cdot (\boldsymbol{\Gamma}^H \mathbf{A}^H \mathbf{A} \boldsymbol{\Gamma}) \circ \mathbf{R}^T_{\overset{\smile}{s}\tilde{s}} \tag{41}$$

$$\mathbf{I}_{\mathbf{f}_D\mathbf{f}_D} = N \cdot (\boldsymbol{\Gamma}^H \mathbf{A}^H \mathbf{A} \boldsymbol{\Gamma}) \circ \mathbf{R}^T_{\overset{\smile}{s}\overset{\smile}{s}} \tag{42}$$

where $\dot{\mathbf{A}} = [\frac{\partial \mathbf{a}(\theta_1)}{\partial \theta_1}, \cdots, \frac{\partial \mathbf{a}(\theta_Q)}{\partial \theta_Q}]$, $\dot{\mathbf{\Gamma}}_\xi = [\frac{\partial \gamma_1}{\partial \xi_1}, \cdots, \frac{\partial \gamma_Q}{\partial \xi_q}]$, $\dot{\mathbf{\Gamma}}_\eta = [\frac{\partial \gamma_1}{\partial \eta_1}, \cdots, \frac{\partial \gamma_Q}{\partial \eta_q}]$, $\mathbf{R}_{\widehat{s}\widehat{s}} = \frac{1}{N}\sum_{n=0}^{N-1} \widehat{\mathbf{s}}(n)\widehat{\mathbf{s}}^H(n)$, $\breve{\mathbf{s}}(n) = j2\pi n\widehat{\mathbf{s}}(n)$, $\mathbf{R}_{\breve{s}\widehat{s}} = \frac{1}{N}\sum_{n=0}^{N-1} \breve{\mathbf{s}}(n)\widehat{\mathbf{s}}^H(n)$, $\tilde{\mathbf{s}}(n) = \mathbf{s}_D(\mathbf{f}_D, n) \circ \dot{\mathbf{s}}(\tau, n)$, $\dot{\mathbf{s}}(\tau, n) = [\frac{\partial s_1(n-\tau_1)}{\partial \tau_1}, \cdots, \frac{\partial s_Q(n-\tau_Q)}{\partial \tau_Q}]^T$. Besides, $\mathbf{R}_{\tilde{s}\tilde{s}}$, and $\mathbf{R}_{\breve{s}\tilde{s}}$ have similar definition to $\mathbf{R}_{\widehat{s}\widehat{s}}$ and $\mathbf{R}_{\breve{s}\widehat{s}}$.

Therefore, given the relationship between CRB and the Fisher information matrix, define $\mathbf{\Delta} = \mathbf{I}^{-1}(\boldsymbol{\mu})$, and consequently we have

$$\text{CRB}_\theta = \sqrt{1/Q\sum_{q=1}^{Q} \mathbf{\Delta}_{q,q}} \tag{43}$$

$$\text{CRB}_\gamma = \sqrt{1/Q\sum_{q=1}^{Q} (\mathbf{\Delta}_{Q+q,Q+q} + \mathbf{\Delta}_{2Q+q,2Q+q})} \tag{44}$$

$$\text{CRB}_\tau = \sqrt{1/Q\sum_{q=1}^{Q} \mathbf{\Delta}_{3Q+q,3Q+q}} \tag{45}$$

$$\text{CRB}_{f_D} = \sqrt{1/Q\sum_{q=1}^{Q} \mathbf{\Delta}_{4Q+q,4Q+q}} \tag{46}$$

where CRB_θ, CRB_γ, CRB_τ, and CRB_{f_D} represent the Cramer-Rao bounds for DOAs, complex amplitudes, time delays, and Doppler shifts, respectively. $\mathbf{\Delta}_{p,q}$ denotes the (p, q)th element of $\mathbf{\Delta}$.

Acknowledgments

This work was supported in part by the Natural Science Basic Research Project of Shaanxi Province under Grant 2018JQ6046, in part by the China Postdoctoral Science Foundation under Grant 2017M623123, and in part by the Fundamental Research Funds for the Central Universities of China under Grant XJS18033.

References

[1] H. L. Van Trees, Detection, Estimation, and Modulation Theory, Optimum Array Processing, John Wiley & Sons, 2004.

[2] R. O. Schmidt, Multiple emitter location and signal parameter estimation, IEEE Trans. Antennas Propag. 34 (3) (1986) 276–280.

[3] R. Roy, T. Kailath, ESPRIT-estimation of signal parameters via rotational invariance techniques, IEEE Trans. Acoust., Speech, Signal Process., 37 (7) (1989) 984–995.

[4] F.-G. Yan, L. Shuai, J. Wang, J. Shi, M. Jin, Real-valued root-MUSIC for DOA estimation with reduced-dimension EVD/SVD computation, Signal Process. 152 (2018) 1 – 12.

[5] M. Sun, Y. Wang, J. Pan, Direction of arrival estimation by modified orthogonal propagator method with linear prediction in low SNR scenarios, Signal Process. 156 (2019) 41 – 45.

[6] D. Malioutov, M. Cetin, A. S. Willsky, A sparse signal reconstruction perspective for source localization with sensor arrays., IEEE Trans. Signal Process. 53 (8) (2005) 3010–3022.

[7] Y. Wang, A. Hashemi-Sakhtsari, M. Trinkle, B. W.-H. Ng, Sparsity-aware DOA estimation of quasi-stationary signals using nested arrays, Signal Process. 144 (2018) 87 – 98.

[8] R. Zheng, X. Xu, Z. Ye, T. H. A. Mahmud, J. Dai, K. Shabir, Sparse Bayesian learning for off-grid DOA estimation with gaussian mixture

priors when both circular and non-circular sources coexist, Signal Process. 161 (2019) 124 – 135.

[9] J. Ward, J. R. T. Compton, Improving the performance of a slotted ALOHA packet radio network with an adaptive array, IEEE Trans. Commun. 40 (2) (1992) 292–300.

[10] A. Jakobsson, A. L. Swindlehurst, P. Stoica, Subspace-based estimation of time delays and Doppler shifts, IEEE Trans. Signal Proces. 46 (9) (1998) 2472–2483.

[11] J. Li, R. Compton, Maximum likelihood angle estimation for signals with known waveforms, IEEE Trans. Signal Process. 41 (9) (1993) 2850–2862.

[12] J. Li, B. Halder, P. Stoica, M. Viberg, Computationally efficient angle estimation for signals with known waveforms, IEEE Trans. Signal Process. 43 (9) (1995) 2154–2163.

[13] A. L. Swindlehurst, Time delay and spatial signature estimation using known asynchronous signals, IEEE Trans. Signal Proces. 46 (2) (1998) 449–462.

[14] N. Wang, P. Agathoklis, A. Antoniou, A new DOA estimation technique based on subarray beamforming, IEEE Trans. Signal Process. 54 (9) (2006) 3279–3290.

[15] J.-F. Gu, S. C. Chan, W.-P. Zhu, M. Swamy, DOA estimation and tracking for signals with known waveform via symmetric sparse subarrays, in: 2012 IEEE 55th Int. Midwest Symp. Circuits Syst. (MWSCAS), IEEE, 2012, pp. 952–955.

[16] J.-F. Gu, W.-P. Zhu, M. Swamy, Sparse linear arrays for estimating and tracking DOAs of signals with known waveforms, in: 2013 IEEE Int. Symp. Circuits Syst. (ISCAS), IEEE, 2013, pp. 2187–2190.

[17] J.-F. Gu, W.-P. Zhu, M. Swamy, Fast and efficient DOA estimation method for signals with known waveforms using nonuniform linear arrays, Signal Process. 114 (2015) 265–276.

[18] J.-F. Gu, W.-P. Zhu, M. Swamy, Direction of arrival tracking for signals with known waveforms based on block least squares techniques, J. Frankl. Inst. 354 (11) (2017) 4573–4594.

[19] M. Cedervall, R. L. Moses, Efficient maximum likelihood DOA estimation for signals with known waveforms in the presence of multipath, IEEE Trans. Signal Process. 45 (3) (1997) 808–811.

[20] H. Li, G. Liu, J. Li, Angle estimator for signals with known waveforms, Electron. Lett. 35 (23) (1999) 1992–1994.

[21] L. N. Atallah, S. Marcos, DOA estimation and association of coherent multipaths by using reference signals, Signal Process. 84 (6) (2004) 981–996.

[22] J.-F. Gu, P. Wei, H.-M. Tai, Fast direction-of-arrival estimation with known waveforms and linear operators, IET Signal Process. 2 (1) (2008) 27–36.

[23] Y.-Y. Dong, C. Dong, W. Liu, M.-M. Liu, Z. Tang, A structure-aware DOA estimation method for sources with short known waveforms, IEEE Access 6 (2018) 71271–71278.

[24] Y.-Y. Dong, C.-X. Dong, W. Liu, M.-M. Liu, Z.-Z. Tang, Robust DOA estimation for sources with known waveforms against Doppler shifts via oblique projection, IEEE Sensors J. 18 (16) (2018) 6735–6742.

[25] W. Sun, Y.-X. Yuan, Optimization Theory and Methods–Nonlinear Programming, Springer, 2006.

[26] S. M. Kay, Fundamentals of Statistical Signal Processing, Prentice Hall PTR, 1993.

[27] H. Chen, W. Liu, W.-P. Zhu, M. Swamy, Q. Wang, Mixed rectilinear sources localization under unknown mutual coupling, J. Frankl. Inst. 356 (4) (2019) 2372 – 2394.